Article

Floating under a levitating liquid

https://doi.org/10.1038/s41586-020-2643-8

Received: 25 March 2020

Accepted: 10 July 2020

Published online: 2 September 2020

Check for updates

Benjamin Apffel[1,3], Filip Novkoski[1,3], Antonin Eddi[2] & Emmanuel Fort[1]✉

When placed over a less dense medium, a liquid layer will typically collapse downwards if it exceeds a certain size, as gravity acting on the lower liquid interface triggers a destabilizing effect called a Rayleigh–Taylor instability[1,2]. Of the many methods that have been developed to prevent the liquid from falling[3–6], vertical shaking has proved to be efficient and has therefore been studied in detail[7–13]. Stabilization is the result of the dynamical averaging effect of the oscillating effective gravity. Vibrations of liquids also induce other paradoxical phenomena such as the sinking of air bubbles[14–19] or the stabilization of heavy objects in columns of fluid at unexpected heights[20]. Here we take advantage of the excitation resonance of the supporting air layer to perform experiments with large levitating liquid layers of up to half a litre in volume and up to 20 centimetres in width. Moreover, we predict theoretically and show experimentally that vertical shaking also creates stable buoyancy positions on the lower interface of the liquid, which behave as though the gravitational force were inverted. Bodies can thus float upside down on the lower interface of levitating liquid layers. We use our model to predict the minimum excitation needed to withstand falling of such an inverted floater, which depends on its mass. Experimental observations confirm the possibility of selective falling of heavy bodies. Our findings invite us to rethink all interfacial phenomena in this exotic and counter-intuitive stable configuration.

Maintaining a liquid upside down is challenging but various situations in which the inverted liquid can be sustained are known. In the case of a limited surface size, capillary forces have a stabilizing effect[21–23]. Alternatively, for large but thin liquid layers suspended under a plate, capillarity opposes gravity[24,25]. In the latter case, the liquid interface does not stay flat but is destabilized in a regular pattern of hanging droplets. This instability driven by gravity, known as the Rayleigh–Taylor instability, occurs at the interface between two fluids whenever a denser fluid is placed over a lighter one[1,2]. Several approaches have been used to stabilize liquid layers, such as temperature gradients[3], electric[4] or magnetic fields[5], rotational motion[6] and vertical vibrations[7–13]. When using vertical vibrations, the amplitude of the vibration must increase with the surface size. The maximum amplitude is set by the triggering of another instability—the Faraday instability—which tends to destabilize fluid surfaces above a certain acceleration threshold[26,27]. However, this threshold can be raised by increasing the fluid viscosity[28]. Hence, the volume of the upside-down liquid can be large, provided the viscosity is suitably chosen.

The vertical vibration of a fluid also induces air bubbles to sink below a certain depth in the liquid, defying the well known Archimedes' principle[14–20]. This effect has been studied for industrial applications in gas holdup and mixing in bubble column reactors[29].

Here we investigate the effect of the vertical vibrations on the buoyancy of bodies immersed in levitating liquid layers and in particular at their lower interface. Our experimental setup consists of a plexiglass container fixed on a shaker that vibrates vertically at a frequency of $\omega/(2\pi)$ and with amplitude A (Fig. 1a). The container is filled with silicon oil or glycerol with high viscosity (typically ranging from 0.2 Pa s to 1 Pa s) to increase the Faraday instability threshold[8]. Though they have different physical properties, both liquids exhibit similar behaviour provided that their viscosity is large enough. In particular, the wetting conditions appear to have limited influence, owing to dynamical effects on the contact line. Air bubbles are observed to sink when placed below a critical depth. This behaviour, which defies standard buoyancy, can be explained by a simple model that takes into account the kinetic force—also called the Bjerknes force[30]—that is exerted on the bubble in the oscillating bath[14,16] (see Supplementary Materials and Supplementary Video 1 for details). By expanding an already sunken bubble, we create an air layer trapped below a levitated liquid layer (Fig. 1b and Supplementary Video 2). The lower interface of the liquid layer is stabilized by the vertical shaking, preventing the release of the trapped air. This air layer acts as a vertical spring loaded with the liquid mass placed upon it and driven by the shaker (Fig. 1c). It can be modelled by a driven damped harmonic oscillator $\ddot{z} + 2\Gamma\omega_{res}\dot{z} + \omega_{res}^2 z = A\omega^2\cos(\omega t)$ where ω_{res} is the resonance frequency of the air layer and Γ is the damping ratio due to the shearing induced by the relative motion between the levitating liquid layer and the bath walls (see Supplementary Information). In the laboratory frame (denoted by subscript 'l'), the normalized oscillation amplitude $A_l(\omega)/A$ and its associated relative phase $\phi_l(\omega) - \phi$ compared to the shaker clearly show the expected resonance behaviour (Fig. 1c, d). The air layer thus enables the enhancement of the excitation amplitude of the shaker by more than one order of magnitude. Near resonance, the amplitude is high enough to excite the Faraday instability on both sides of the fluid layer (see Fig. 1d, inset, and Supplementary Video 3). The resulting 'rain' emitted from the lower interface induces a thinning of the fluid layer which can be avoided by reducing the excitation amplitude. Provided that the

[1]ESPCI Paris, PSL University, CNRS, Institut Langevin, Paris, France. [2]PMMH, CNRS, ESPCI Paris, Université PSL, Sorbonne Université, Université de Paris, Paris, France. [3]These authors contributed equally: Benjamin Apffel, Filip Novkoski. ✉e-mail: emmanuel.fort@espci.fr

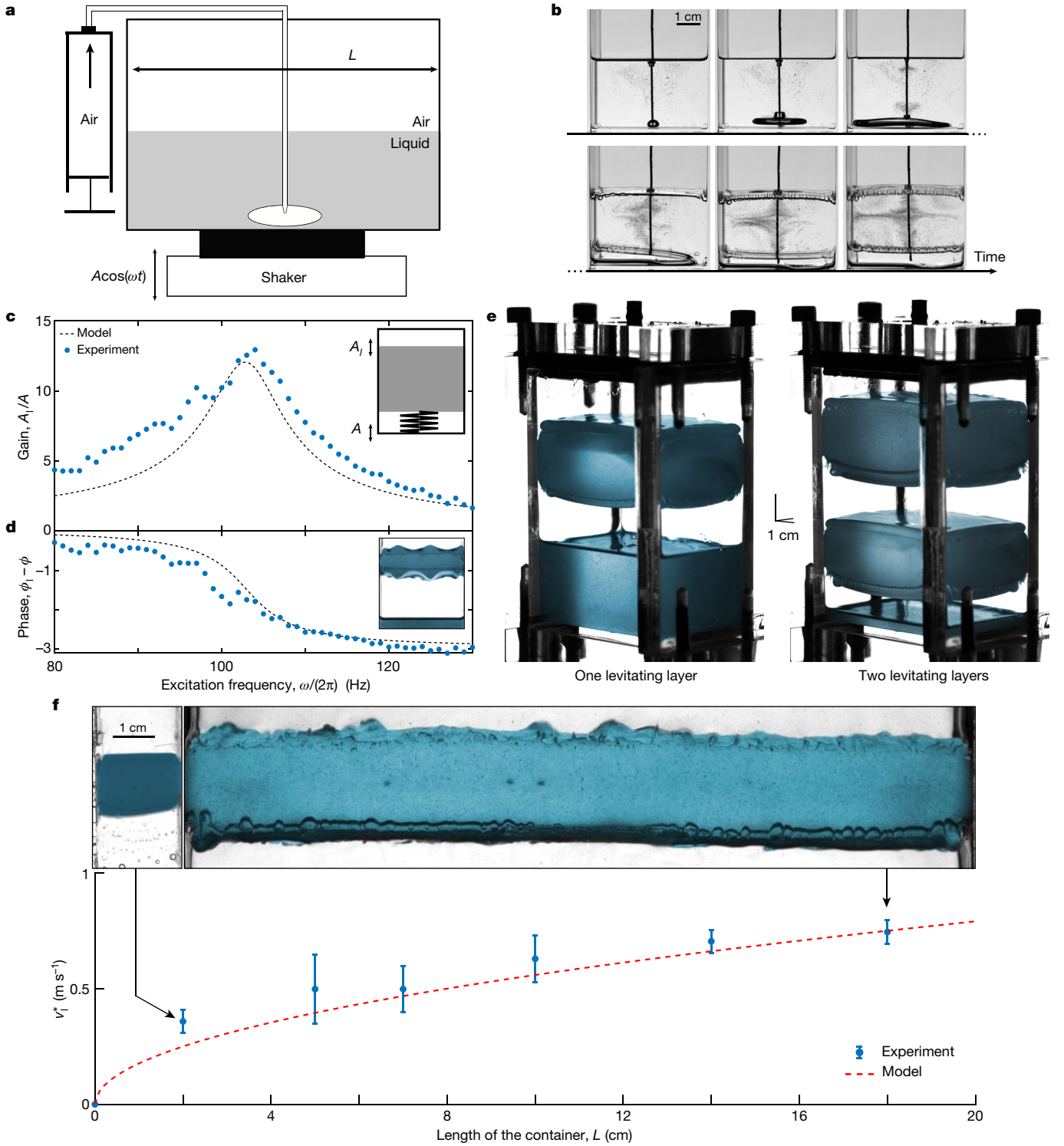

Fig. 1 | Levitating liquid layer stabilized by the Kapitza effect. **a**, Experimental setup, composed of a plexiglass container of various sizes (up to 20 cm in width) attached on a vertically oscillating shaker with amplitude A and frequency $\omega/(2\pi)$. The liquid is either glycerol or silicon oil with high viscosity (typically 0.5 Pa s). The bubbles are created by injecting air with a syringe through a long needle. We operate at room temperature (20 °C). **b**, Image sequence (left to right, top to bottom) of the creation of the air layer obtained by injecting air at the bottom of the oscillating liquid bath through a needle. The sinking bubble grows until it completely fills the bottom of the bath (see Supplementary Videos 1, 2). **c**, **d**, Vertical amplitude of the liquid layer, A_l/A (**c**), and the relative phase shift $\phi_l - \phi$ of the liquid oscillations compared with that of the shaker (**d**) as a function of the excitation frequency $\omega/(2\pi)$. Insets, schematic of the spring–mass system composed of the air layer loaded with the levitating liquid (**c**) and image of the Faraday instability that is triggered on the two opposite surfaces of the levitating liquid layer of silicon oil (**d**; see Supplementary Video 3). The experimental data (full circles) are fitted by the spring–mass model with fitting parameters $\omega/(2\pi) = 103$ Hz and $\Gamma = 0.04$ (dashed line; see Supplementary Information for details). **e**, Digitally colourized three-quarter views of the oscillating containers with one and two levitating liquid layers of silicon oil (see Supplementary Video 4). **f**, Top, Digitally colourized side views of the levitating bath in containers of widths $L = 2$ cm (left) and $L = 18$ cm (right); see Supplementary Video 5. Bottom, critical liquid velocity $v_l^* = A_l\omega$ for Kapitza stabilization of the liquid layer as a function of the width L of the container: experimental data (circles) and model $v_l^* = \sqrt{gL/\pi}$ (dashed line). Error bars correspond to extremal values over five experiments.

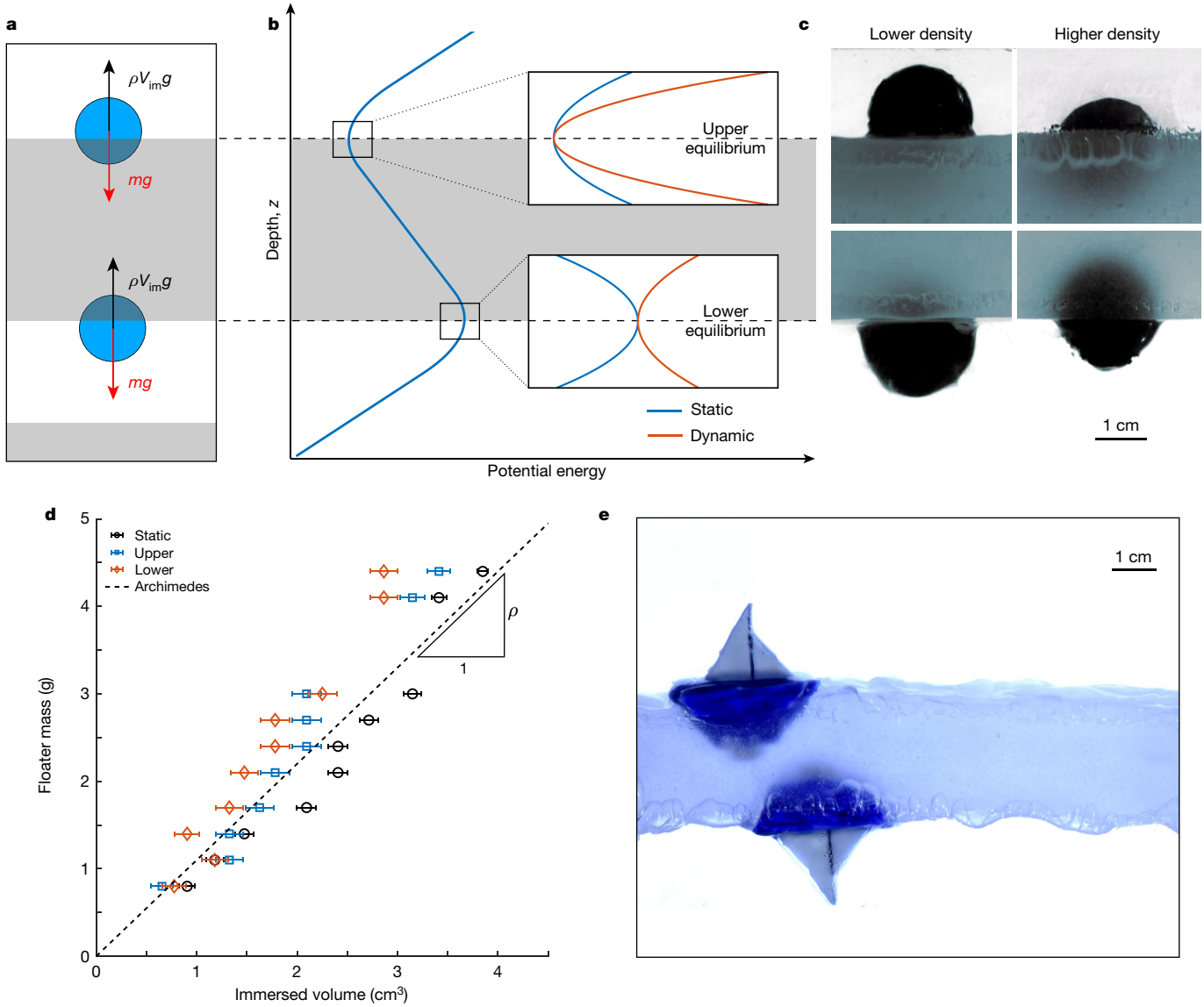

Fig. 2 | Archimedes' principle over and under a levitating liquid layer. **a**, Schematic of the force balance at the two opposing interfaces; the buoyant force cancels the weight of the immersed bodies, where V_{im} is the immersed volume. **b**, Typical profile of the static potential (blue) along the vertical direction z neglecting the dynamical effects. Two equilibrium positions appear at each interface; the lower equilibrium is unstable. Insets, magnifications of the potential near the equilibrium positions with the addition of the dynamical stabilizing effect (red line; see Supplementary Information). **c**, Digitally colourized side views of plastic spheres 2 cm in diameter, floating upwards and downwards with lower (left) and higher density (right). **d**, Time-averaged equilibrium positions for spheres 2 cm in diameter with varying masses, as a function of the immersed volume at the upper interface (blue squares) and the lower interface (red diamonds). Black circles give the equilibrium positions obtained without shaking. The dashed line is given by the Archimedes' principle with experimentally measured $\rho_l = 1.1\,\mathrm{kg\,l^{-1}}$ for glycerol. The error bars correspond to extremal values over three measurements. **e**, Boats floating above and below a levitated liquid layer (see Supplementary Video 6; digitally colourized).

spring–mass oscillation is properly tuned, there is no restriction on the number of levitating layers that can be sustained on top of one another (see Fig. 2e and Supplementary Video 4).

As mentioned, the vertical vibrations have a stabilizing effect on the lower fluid interface. This can be interpreted as a Kapitza effect, which is the dynamical stabilization of an inverted pendulum by vertical shaking[31,32]. Solving the Bernoulli equation for the fluid shows that the interface height $\zeta(k)$ at the spatial wavenumber k behaves like an inverted pendulum. The spatial mode satisfies $\ddot{\zeta} + [\omega_0^2(k) + (A_l^2 k^2 \omega^2)/2]\zeta = 0$ with $\omega_0^2(k) = -gk + (\gamma k^3)/\rho_l$ the gravito-capillary dispersion relation with inverted gravity, and ρ_l the density of the liquid and γ its surface tension. Without vibrations, the oscillator is unstable for small enough k ($\omega_0^2(k) < 0$), leading to the Rayleigh–Taylor instability, whereas large wave numbers are stabilized by capillarity. The last term in the equation arises from the modulation of the effective gravity. In a gravitational regime, the stabilization is reached for wavenumbers satisfying $k > 2g/(A_l^2\omega^2)$ (see Supplementary Information). The limited width L for the bath sets a maximum limit for the observed excitable wavenumber $k > 2\pi/L$ (only antisymmetric modes satisfying volume conservation are considered). As a consequence, the stability of the interface is obtained for oscillating liquid velocities $v_l = A_l\omega$ above a critical velocity $v_l^* = \sqrt{gL/\pi} < v_l$. There seems to be no size limit for stabilization. The maximum levitated mass was 0.5 l in a 12 × 12 cm² container, and the maximum width achieved was 20 cm. The limitations in mass are due only to the shaker. In addition, no decay in time was observed and the layers remained stable for arbitrarily long times. Figure 1f shows the critical oscillating velocity v_l^* needed to stabilize baths with widths L up to 18 cm (the insets show views of levitating layers for bath widths

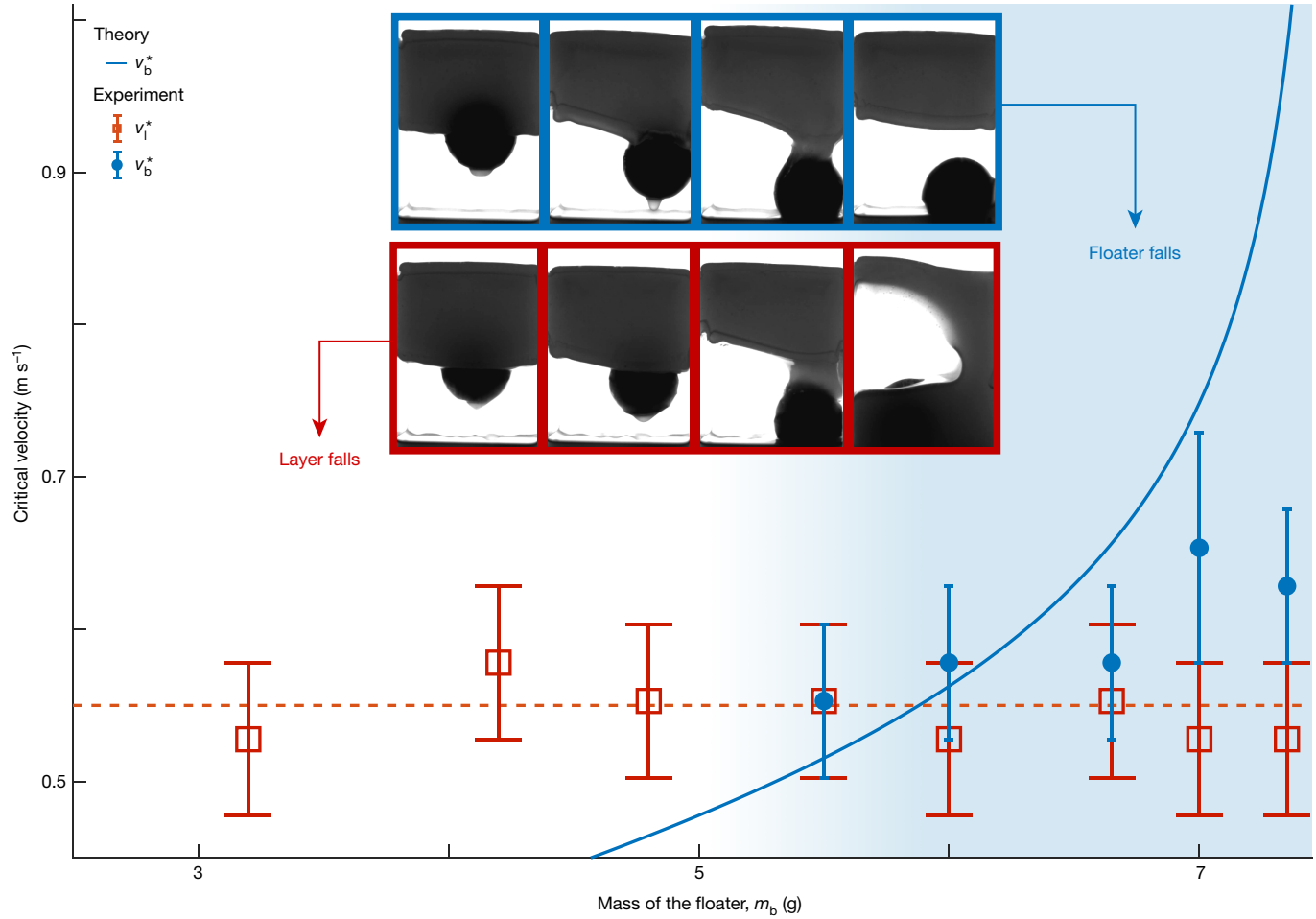

Fig. 3 | Stability of the floater and the liquid layer. Critical velocities for the stability of the liquid layer v_l^* and for the floater v_b^* as a function of the floater mass m_b. The experiments are performed in a $4 \times 5\,cm^2$ container with silicon oil and spherical floaters with a diameter of 2.5 cm with various masses. The model (blue line), which is based on dynamic stabilization, uses the experimentally measured liquid density, $\rho = 0.92\,kg\,l^{-1}$, and no adjustable parameters. Above a certain floater mass $v_b^* > v_l^*$ (blue area) the floater can fall while the liquid layer remains stable. The error bars correspond to extremal values over three measurements. The dashed red line is the mean value of the v_l^* measurements. Inset, image sequences (left to right) of the experiment showing the layer falling at v_l^* for a floater mass of $m_b = 4.8$ g and showing the floater falling at v_b^* for $m_b = 6.6$ g (see Supplementary Video 7).

$L = 2$ cm and $L = 18$ cm; see Supplementary Video 5). Other effects might have an influence on the stability, such as friction or the flows formed at the boundary, but their influence is limited (see Supplementary Information).

We now focus on objects floating at the inverted interface of the levitating fluid layer. Archimedes' principle states that the upward buoyant force exerted on an immersed body, whether fully or partially submerged, is equal to the weight of the displaced fluid. Although it may seem counterintuitive, the transpose symmetric position at the lower interface (see Fig. 2a) also exhibits an upward buoyant force equal to the weight of displaced liquid. Figure 2b shows the typical potential exerted on a floating body without taking into account the dynamical effects (see Supplementary Information for details). The two equilibrium positions associated with each interface are clearly visible. However, although the upper position is stable, the lower is not: pushing the body down (or up) would make it fall (or float to the upper interface). Taking into account the dynamical effect—that is, the time-averaged effect of the oscillations—provides an additional stabilizing dynamical potential around the two equilibrium positions (see Fig. 2b, inset). Averaged small displacements Z_b of the floater around the two equilibrium positions satisfy the same dynamical equation $\ddot{Z}_b + \omega_b^2(1+\alpha)Z_b = 0$, where ω_b is the angular frequency associated with the buoyancy force and $\alpha = \frac{\omega_b^2}{2}\left(\frac{A_l\omega}{g}\right)^2$ is the correction induced by the averaged dynamical effects (see Supplementary Information for details). Although the dynamical effects increase the stability of the equilibrium at the upper interface ($\omega_b^2 > 0$, $\alpha > 0$), the unstable static equilibrium at the lower interface ($\omega_b^2 < 0$) is stabilized by the dynamical effects ($\alpha < 0$). It is interesting to note that similar dynamical stabilizations were observed with a washer mounted on a vibrated inverted pendulum[20]. The floater stability is reached for liquid velocity v_l above a critical value given by $v_b^* = \sqrt{2}g/|\omega_b| < v_l$. It is thus possible to have floating bodies with varying densities above and below the levitating liquid layers (see Fig. 2c). Hence the vibration not only gives stability of the lower horizontal interface of a liquid but also permits vertical stabilization of the unstable equilibrium position that a floater would experience on such interface. This dynamical 'anti-gravity' enables boats to float on both interfaces (Fig. 2e, see Supplementary Video 6)[33]. Note that the drag force induced by secondary flows—which we see as recirculation in the liquid layer—should not considerably change the vertical equilibrium position (see Supplementary Video 2 and Supplementary Information).

These stability conditions suggest that the critical fluid velocity to stabilize a floater v_b^* and the liquid layer v_l^* are different, and that sufficiently massive floaters should fall before the layer collapses ($v_b^* > v_l^*$). We performed the experiments in silicon oil with spherical floaters of increasing mass; the heaviest floater had almost neutral buoyancy (Fig. 3). In contrast to light floaters, which fall with the liquid layer as

the excitation amplitude is decreased, heavier floaters fall before the levitating layer is destabilized (see Fig. 3, inset, and Supplementary Video 7). The theoretical critical velocity v_b^* can be exactly computed for spheres without any adjustable parameters (solid blue line). The expected range of masses for which $v_b^* > v_l^*$ is consistent with the experimental findings (Fig. 3, blue shaded region) and the values v_b^* are in reasonable agreement. Discrepancy occurs for almost neutrally buoyant floaters (as also for buoyant equilibrium position). In this limit, new phenomena are observed, such as a small relative motion of floaters with respect to the surrounding fluid layer, which seems to have an important role in the floater equilibrium.

This counter-intuitive upside-down buoyancy phenomenon suggests that the stabilization of Rayleigh–Taylor instability through vibrations can be considered not only in itself but also as offering opportunities for new experiments in unexplored conditions. We anticipate that phenomena that occur at the interface between air and liquids—such as transport and segregation—could be investigated and reformulated in this exotic configuration.

Online content

Any methods, additional references, Nature Research reporting summaries, source data, extended data, supplementary information, acknowledgements, peer review information; details of author contributions and competing interests; and statements of data and code availability are available at https://doi.org/10.1038/s41586-020-2643-8.

1. Lord Rayleigh. Investigation of the character of the equilibrium of an incompressible heavy fluid of variable density. *Proc. Lond. Math. Soc.* **14**, 170–177 (1883).
2. Lewis, D. J. The instability of liquid surfaces when accelerated in a direction perpendicular to their planes. II. *Proc. R. Soc. Lond. A* **202**, 81–96 (1950).
3. Burgess, J. M., Juel, A., McCormick, W. D., Swift, J. B. & Swinney, H. L. Suppression of dripping from a ceiling. *Phys. Rev. Lett.* **86**, 1203–1206 (2001).
4. Cimpeanu, R., Papageorgiou, D. T. & Petropoulos, P. G. On the control and suppression of the Rayleigh–Taylor instability using electric fields. *Phys. Fluids* **26**, 022115 (2014).
5. Rannacher, D. & Engel, A. Suppressing the Rayleigh–Taylor instability with a rotating magnetic field. *Phys. Rev. E* **75**, 016311 (2007).
6. Tao, J. J., He, X. T., Ye, W. H. & Busse, F. H. Nonlinear Rayleigh–Taylor instability of rotating inviscid fluids. *Phys. Rev. E* **87**, 013001 (2013).
7. Wolf, G. H. The dynamic stabilization of the Rayleigh–Taylor instability and the corresponding dynamic equilibrium. *Z. Phys.* **227**, 291–300 (1969).
8. Wolf, G. H. Dynamic stabilization of the interchange instability of a liquid–gas interface. *Phys. Rev. Lett.* **24**, 444–446 (1970).
9. Lapuerta, V., Mancebo, F. J. & Vega, J. M. Control of Rayleigh–Taylor instability by vertical vibration in large aspect ratio containers. *Phys. Rev. E* **64**, 016318 (2001).
10. Kumar, S. Mechanism for the Faraday instability in viscous liquids. *Phys. Rev. E* **62**, 1416–1419 (2000).
11. Pototsky, A. & Bestehorn, M. Faraday instability of a two-layer liquid film with a free upper surface. *Phys. Rev. Fluids* **1**, 023901 (2016).
12. Pototsky, A., Oron, A. & Bestehorn, M. Vibration-induced floatation of a heavy liquid drop on a lighter liquid film. *Phys. Fluids* **31**, 087101 (2019).
13. Sterman-Cohen, E., Bestehorn, M. & Oron, A. Rayleigh–Taylor instability in thin liquid films subjected to harmonic vibration. *Phys. Fluids* **29**, 052105 (2017); correction **29**, 109901 (2017).
14. Baird, M. H. I. Resonant bubbles in a vertically vibrating liquid column. *Can. J. Chem. Eng.* **41**, 52–55 (1963).
15. Jameson, G. J. The motion of a bubble in a vertically oscillating viscous liquid. *Chem. Eng. Sci.* **21**, 35–48 (1966).
16. Sorokin, V. S., Blekhman, I. I. & Vasilkov, V. B. Motion of a gas bubble in fluid under vibration. *Nonlinear Dyn.* **67**, 147–158 (2012).
17. Blekhman, I. I., Blekhman, L. I., Vaisberg, L. A., Vasil'kov, V. B. & Yakimova, K. S. "Anomalous" phenomena in fluid under the action of vibration. *Dokl. Phys.* **53**, 520–524 (2008).
18. Blekhman, I. I., Blekhman, L. I., Sorokin, V. S., Vasilkov, V. B. & Yakimova, K. S. Surface and volumetric effects in a fluid subjected to high-frequency vibration. *Proc. Inst. Mech. Eng. C* **226**, 2028–2043 (2012).
19. Zen'kovskaja, S. M. & Novosjadlyj, V. A. Vlijanie vertikal'nyh kolebanij na dvuhslojnuju sistemu s deformiruemoj poverhnost'ju razdela [Influence of vertical oscillations on a bilaminar system with a non-rigid interface.] *Zh. Vychisl. Mat. Mat. Fiz.* **48**, 1710–1720 (2008).
20. Chelomei, V. N. Mechanical paradoxes caused by vibrations. *Sov. Phys. Dokl.* **28**, 387–390 (1983).
21. Young, T. III. An essay on the cohesion of fluids. *Philos. Trans. R. Soc. Lond.* **95**, 65–87 (1805).
22. Thomson, W. LX. On the equilibrium of vapour at a curved surface of liquid. *Lond. Edinb. Dublin Philos. Mag. J. Sci.* **42**, 448–452 (1871).
23. de Gennes, P.-G., Brochard-Wyart, F. & Quere, D. *Capillarity and Wetting Phenomena: Drops, Bubbles, Pearls, Waves* (Springer Science & Business Media, 2013).
24. Fermigier, M., Limat, L., Wesfreid, J. E., Boudinet, P. & Quilliet, C. Two-dimensional patterns in Rayleigh–Taylor instability of a thin layer. *J. Fluid Mech.* **236**, 349–383 (1992).
25. Myshkis, A. D., Babskii, V. G., Kopachevskii, N. D., Slobozhanin, L. A. & Tyuptsov, A. *Low-Gravity Fluid Mechanics. Mathematical Theory of Capillary Phenomena* (Springer, 1987).
26. Faraday, M. On a peculiar class of acoustical figures; and on certain forms assumed by groups of particles upon vibrating elastic surfaces. *Philos. Trans. R. Soc. Lond.* **121**, 299–340 (1831).
27. Douady, S. Experimental study of the Faraday instability. *J. Fluid Mech.* **221**, 383–409 (1990).
28. Kumar, K. & Tuckerman, L. S. Parametric instability of the interface between two fluids. *J. Fluid Mech.* **279**, 49–68 (1994).
29. Elbing, B. R., Still, A. L. & Ghajar, A. J. Review of bubble column reactors with vibration. *Ind. Eng. Chem. Res.* **55**, 385–403 (2016).
30. Bjerknes, V. F. K. *Fields of Force: Supplementary Lectures, Applications to Meteorology* (Columbia Univ. Press and Macmillan, 1906).
31. Kapitza, P. L. Dynamic stability of a pendulum when its point of suspension vibrates. *Sov. Phys. JETP* **21**, 588–597 (1951).
32. Krieger, M. S. Interfacial fluid instabilities and Kapitsa pendula. *Eur. Phys. J. E* **40**, 67 (2017).
33. Landau, L. D. & Lifshitz, E. M. *Mechanics* (Pergamon, 1969).

Data availability

All the datasets generated during the current study are available in the Supplementary Information.

Acknowledgements We thank S. Protière, A. Lazarus, S. Wildeman and the staff and students of 'Projets Scientifiques en Equipes' for insightful discussions. We thank the AXA research fund and the French National Research Agency LABEX WIFI (ANR-10-LABX-24) for support.

Author contributions All the authors discussed, interpreted the results and conceived the theoretical framework. E.F. devised the initial idea. B.A. and F.N. designed and performed the experiments. B.A., F.N. and E.F. wrote the paper. All authors reviewed the manuscript.

Competing interests The authors declare no competing interests.

Additional information
Supplementary information is available for this paper at https://doi.org/10.1038/s41586-020-2643-8.
Correspondence and requests for materials should be addressed to E.F.
Peer review information *Nature* thanks Koji Hasegawa, Vladislav Sorokin and the other, anonymous, reviewer(s) for their contribution to the peer review of this work. Peer reviewer reports are available.
Reprints and permissions information is available at http://www.nature.com/reprints.